Low-frequency spin dynamics in diluted magnetic semiconductors

Huu-Nha Nguyen [1] and Van-Nham Phan [2,3,*]

[1] *Department of Theoretical Physics, VNUHCM-University of Science, 227 Nguyen Van Cu, Ho Chi Minh City, Vietnam*

[2] *Institute of Research and Development, Duy Tan University, 3 Quang Trung, Danang 550000, Vietnam*

[3] *Faculty of Natural Sciences, Duy Tan University, 3 Quang Trung, Danang 550000, Vietnam*

(Received 5 July 2022; revised 8 February 2023; accepted 31 March 2023; published 7 April 2023)

The low-frequency dynamical magnetic properties in paramagnetic diluted magnetic semiconductors are addressed in the framework of the dynamical mean-field theory applied for the Kondo lattice model. In the infinite-dimensional limit, a set of self-consistent equations is derived so the single-particle Green's function and its self-energy can be evaluated numerically. In terms of the Green's function and self-energies, the local dynamical spin susceptibility function and then the spin-relaxation rate are explicitly expressed based on the Baym-Kadanoff approach. It is found that the spin fluctuations become dominated, indicated by the sharp peak appearing at the low frequency of the spin dynamical susceptibility function in the case of large magnetic coupling and temperature close to the paramagnetic-ferromagnetic transition point. The low-frequency spin dynamic in the systems is also addressed in the signatures of the spin-relaxation process. In the case of large temperature and small magnetic coupling, the spin-relaxation rate releases the scenario of the Korringa process specifying the weak correlation systems likely normal metals. Otherwise, i.e., at small temperature and large magnetic coupling, we find exponential behavior of the spin-relaxation rate versus temperature. Moreover, at a temperature approaching the paramagnetic-ferromagnetic transition point, one finds sharp suppression of the spin-relaxation rate or speeding up of the spin-relaxation time. These scenarios are attributed to the appearance of the magnetic coherence bound state or the spin clusters in diluted magnetic semiconductors due to the strongly magnetic correlations.

DOI: 10.1103/PhysRevB.107.155113

I. INTRODUCTION

Spin dynamics in diluted magnetic semiconductors (DMSs) is one of the most stimulating issues that attracts much interest because of its potential to understand the nature of magnetic signatures and prospective applications in future spintronics [1,2]. In DMS materials, magnetic (e.g., Mn) ions are lightly doped into a semiconducting host. According to the chemical structure of the semiconducting host, one categorizes II-VI or III-V Mn-based DMSs [3]. In II-VI Mn-based DMSs, Mn is divalent with high spin configuration. The spin-dependent hybridization between anion p and Mn d states leads to superexchange, a short-range antiferromagnetic coupling among the Mn moments [4]. The competition between the ferromagnetic and antiferromagnetic interactions may lead to the spin-glass phase [5]. Meanwhile, in the III-V Mn-based DMSs, the antiferromagnetic superexchange is overruled by carrier-mediated ferromagnetic interactions. With the completely different signatures in the ground state, the spin dynamic properties of the two categories of DMSs are significantly different [1–3,6]. In the present study, we consider the spin dynamics in III-V Mn-based DMS materials as a pioneer work. In this aspect, the ferromagnetic (FM) state is stabilized in the system if the temperature is sufficiently small [7–12]. Increasing the temperature might fluctuate the magnetic ordering and the system would be in the paramagnetic (PM) state. The magnetic properties in the system could be interpreted in the mechanism of the Zener kinetic exchange, the s-f, p-d exchange, or the Kondo lattice model (KLM) [1,2,6,7,13,14], and in the strong-coupling limit, that might reduce to the double-exchange model usually applicable in doped manganites [2,15]. The KLM was originally introduced to model the heavy fermion systems [16] and it has been widely applied to III-V Mn-based DMSs, sometimes referred to as the ferromagnetic KLM describing the ferromagnetic coupling between the itinerant carriers and localized magnetic moments at certain lattice sites [15,17–19]. In the framework of the ferromagnetic KLM we have addressed various aspects of the spin dynamical properties in the III-V Mn-based DMSs [20–22].

To understand the characteristics of the PM-FM transition in DMSs, a formation of short-range magnetic order of bound magnetic polarons has been proposed [9–12,21,23]. However, in these studies, the dynamics properties of the system around the transition points have not been mentioned. In the meanwhile, understanding the signatures of the spin fluctuations in the PM state is essential in elucidating the mechanism of the FM transition in a magnetic system. One of the most typical processes possibly inspecting the spin fluctuations is spin relaxation. The spin relaxation describes the relaxation of a nonequilibrium spin population towards equilibrium, characterized by a spin-lattice relaxation time T_1, the time it takes the longitudinal magnetization to reach equilibrium. In the

*Corresponding author: phanvannham@duytan.edu.vn

discussion hereafter, T_1 can be understood as the Korringa relaxation time of nuclear spins [24,25]. The inverse of the spin-relaxation time, $1/T_1$, is the so-called relaxation rate. The spin-relaxation process is driven by spin-orbit and/or spin-spin interactions. In the present study, we simplify the problem by neglecting a feature of the orbital ordered state in DMSs, and so only the spin relaxation caused due to the spin-exchange interaction between localized magnetic ions and carriers is taken into account. The later so-called Korringa relaxation mechanism is applicable in metallic DMSs [26]. In experiment, probing the spin relaxation in CdMnTe DMS has been performed a long time ago by using modulated Faraday rotation or a time domain magnetic spectrometer [27,28], or most recently, by utilizing the spin-flip Raman-scattering technique applied for GaMnAs DMS [29,30]. The observations release the dominant spin fluctuations of the hole ensemble in the PM state. However, the experimental data for the spin-relaxation process in DMSs up to now is still scarce. Meanwhile, to probe the spin-relaxation rate in a strongly correlated electron system, the nuclear magnetic resonance (NMR) technique is also one of the most practicable choices [31]. The Knight shift in NMR has revealed the Korringa contribution to the width of the resonance line in a large number of metallic DMSs (see Ref. [32], and references therein). In theory, the local NMR relaxation rate has been considered in a single-band Hubbard model by utilizing the dynamical mean-field theory (DMFT) [31,33–36] or by using spin-wave and random-phase approximation [37]. In all these studies, the spin-relaxation rate is extracted from a signature of the low-frequency dynamical spin susceptibility function and the results express agreement with the experimental observations [31]. For large magnetic coupling, a DMS is also one of the strongly correlated electron systems [1,2,6]; analyzing the dynamical spin susceptibility function thus is an applicable way to examine the spin-relaxation process in DMSs.

In the present work, the spin-relaxation rate in DMSs is analyzed in the signatures of the dynamical spin susceptibility function in the framework of the DMFT. The DMFT has proven to be a prevailing method dealing with strongly correlated electron systems [38]. Within the limit of infinite-dimensional space, DMFT gives an exact solution and for lower-dimensional cases such as for two- and three-dimensional systems, it delivers a trustworthy approximate result [38,39]. Indeed, experiments with cold atoms in optical lattices have shown that the DMFT leads to reliable results even for finite-dimensional systems [40]. In our present case, the DMS, for instance GaMnAs, has an fcc-lattice structure. In the case of three dimensions ($d = 3$), a number of nearest neighbors of a lattice site is $Z = 12$. The parameter $1/Z$ thus is quite small already and therefore results of the DMFT are applicable for the real DMS systems. The DMFT has been widely used in studying the magnetic properties in DMSs and similar systems [8,21,41,42]. Based on the DMFT, the spin relaxation has been investigated in a single-band Hubbard model [31,33–36]. In our work, the spin-relaxation process is addressed by means of the DMFT applied for the Kondo lattice model. Indeed, the Kondo lattice model has proven to be a consistent microscopic model used to investigate the magnetic properties in DMSs [6]. In the infinite-dimensional limit, we deliver an analytical expression of the dynamical spin susceptibility function based on the Baym-Kadanoff approach [43,44]. Our results reveal that the spin-relaxation rate displays the Korringa law in normal metals for small magnetic coupling and/or in a half-filling impurity band situation. Deviating from that situation, one finds a decrease and a power dependence of the spin-relaxation rate, indicating that the strong magnetic correlations build up even in the PM state. Lowering the temperature decelerates the internal motion corresponding to increasing the spin-relaxation time.

The present paper is organized as follows: In Sec. II we present a microscopic Hamiltonian describing the carrier correlations in the DMSs and its DMFT solution. Section III derives an analytical expression of the dynamical spin susceptibility function based on the Baym-Kadanoff approach. Numerical results and discussions are given in Sec. IV. Finally, a summary and conclusion are outlined in the last section.

II. MODEL AND METHOD

In order to examine the spin fluctuations in III-V Mn-based DMSs, we use here the ferromagnetic KLM [6,15,17–19]. The Hamiltonian of the ferromagnetic KLM describes the ferromagnetic coupling between the itinerant carriers and localized magnetic moments on the same site that can be written as follows:

$$\mathcal{H} = -t \sum_{\langle i,j\rangle\sigma} c^{\dagger}_{i\sigma} c_{j\sigma} + 2J \sum_{i} \alpha_i \mathbf{S}_i \mathbf{s}_i - \mu \sum_{i} n_i, \qquad (1)$$

where $c^{\dagger}_{i\sigma}$ ($c_{i\sigma}$) is the creation (annihilation) operator for an itinerant carrier with spin σ at lattice site i. The first term in the Hamiltonian (1) thus indicates the carrier hopping between the nearest neighbors with amplitude t. In the case of large dimensions d or large numbers of nearest neighbors of a lattice site Z, the hopping term t is often scaled as $t = t^*/\sqrt{2Z}$ and $t^* = 1$ is chosen as a unit of energy [44]. The second term illustrates the Hund magnetic coupling between the spin of itinerent carriers $\mathbf{s}_i = \sum_{\sigma\sigma'} c^{\dagger}_{i\sigma} \boldsymbol{\sigma}_{\sigma\sigma'} c_{i\sigma'}/2$ ($\boldsymbol{\sigma}$ are the Pauli matrices) and the impurity moment $\mathbf{S}_i$ at lattice site i. Note here that the itinerant carrier in the DMSs is the hole [45], hence the ferromagnetic FKM specifies that the magnetic coupling must be positive ($J > 0$) addressing a parallel alignment of itinerant hole and localized spins. In the present study we consider only the Ising type of magnetic coupling; the transversal x and y spin components are ignored. The simplification does not allow any spin-flip processes, which can be important at low temperature where spin-wave excitations may govern the thermodynamics of the system. However, in the present study, spins of itinerant carriers align ferromagnetically with the localized spins, hence the Ising part of the Hund coupling plays a dominant role. Moreover, the essential features of magnetic and electronic properties in DMSs do not depend on whether the exchange is of Ising- or Heisenberg-type coupling [41,46]. In our calculation below, the local moment spin operator is considered as a quantum variable S with two typical values $S = \pm 1$. In most DMSs, the magnitude of localized spin might be larger, for instance $|S| = 5/2$ [2]. However, in the DMFT calculation, the magnitude of the localized spins could be merged with the magnetic coupling constant and renormalized to the unity, i.e., $|S| = 1$. The Green's function,

its self-energy of carriers, and then the physical results are thus unaffected except for a slight change of the magnetic coupling amplitude [47–50]. In the last term, μ is the chemical potential with $n_i = \sum_\sigma c^\dagger_{i\sigma} c_{i\sigma}$ an occupation operator of the itinerant carriers at lattice site i. In the Hamiltonian, a variable α_i is included to express the presence of the magnetic doping at lattice site i, $\alpha = 1(0)$ if site i is occupied (unoccupied) by a magnetic ion. If x is the doping number of the magnetic ions in DMSs, α satisfies a binary distribution function $P(\alpha) = (1-x)\delta(\alpha) + x\delta(1-\alpha)$. In the case of $\alpha_i = 1$ for all i, the Hamiltonian recovers the original Kondo lattice model [8].

In the present work, the Green's function of the itinerant carrier described in Hamiltonian (1) is found by DMFT. In the infinite-dimensional limitation, DMFT delivers an exact solution for the Green's function. We start with the expression of the local one-particle Green's function

$$G_\sigma(i\omega_n) = \int d\varepsilon\, \rho(\varepsilon) \frac{1}{i\omega_n - \varepsilon + \mu - \Sigma_\sigma(i\omega_n)}, \tag{2}$$

where $\omega_n = (2n+1)\pi T$ is the Matsubara frequency at temperature T. In the infinite dimensions, the self-energy $\Sigma_\sigma(i\omega_n)$ is momentum independent, and the noninteracting density of states of the itinerant carriers $\rho(\varepsilon) = \exp(-\varepsilon^2)/\sqrt{\pi}$ is chosen for the hypercubic lattice case. This Green's function can also be determined by solving an effective single-site problem in a dynamical mean field. Based on the Hamiltonian written in Eq. (1), one finds the action for the effective problem

$$\begin{aligned} S_{\text{eff}}(S,\alpha) = &-\int_0^\beta d\tau \int_0^\beta d\tau' \sum_\sigma c^\dagger_\sigma(\tau)\mathcal{G}^{-1}_\sigma(\tau-\tau')c_\sigma(\tau') \\ &+ \int_0^\beta d\tau \sum_\sigma [JS\sigma\alpha - \mu] c^\dagger_\sigma(\tau)c_\sigma(\tau), \end{aligned} \tag{3}$$

with $\mathcal{G}_\sigma(\tau)$ the bare Green's function of the Weiss effective medium written in the imaginary time representation. Note here that we have restricted ourselves to the quantum case of the localized magnetic moment. In this consideration, the magnetic coupling is of Ising type, i.e., only the z component of the spins is of interest. The key idea of the DMFT is that the local one-particle Green's function must in Eq. (2) be considered with one evaluated from the efflective single-site problem, i.e., one has

$$G_\sigma(i\omega_n) = \frac{\partial \mathcal{F}}{\partial \mathcal{G}^{-1}_\sigma(i\omega_n)}, \tag{4}$$

where

$$\mathcal{F} = -\int d\alpha\, P(\alpha) \ln \mathcal{Z}_{\text{eff}}(\alpha) \tag{5}$$

is the free energy of the system and $\mathcal{Z}_{\text{eff}}(\alpha)$ is the partition function of the effective single impurity that can be calculated from the effective action. From Eq. (3), one finds

$$\mathcal{Z}_{\text{eff}}(\alpha) = 2\sum_s \exp\left\{\sum_{n\sigma} \ln \frac{\mathcal{G}^{-1}(i\omega_n) - JS\sigma\alpha}{i\omega_n}\right\}. \tag{6}$$

The local one-particle Green's function thus can be explicitly expressed as

$$G_\sigma(i\omega_n) = \sum_{\alpha S} \frac{W_{\alpha,S}}{Z^{\alpha S}_\sigma(i\omega_n)}. \tag{7}$$

Here $Z^{\alpha S}_\sigma(i\omega_n) = \mathcal{G}^{-1}_\sigma(i\omega_n) - JS\sigma\alpha$ and $W_{\alpha,S}$ ($\alpha = \{0,1\}$) act as the weight factors, that explicitly read

$$W_{0,S} = \frac{2(1-x)}{\mathcal{Z}_{\text{eff}}(0)} \exp \sum_{n\sigma} \ln \frac{\mathcal{G}^{-1}_\sigma(i\omega_n)}{i\omega_n} \tag{8}$$

and

$$W_{1,S} = \frac{2x}{\mathcal{Z}_{\text{eff}}(1)} \exp \sum_{n\sigma} \ln \frac{Z^{\alpha S}_\sigma(i\omega_n)}{i\omega_n}. \tag{9}$$

The weight factors here are not simply a number, they are the functionals of the Green's function. The self-consistency might be closed by using the Dyson equation

$$G^{-1}_\sigma(i\omega_n) = \mathcal{G}^{-1}_\sigma(i\omega_n) - \Sigma_\sigma(i\omega_n). \tag{10}$$

Equations (2), (4), and (10) establish a set of self-consistent equations; the local Green's function of the itinerant carrier and its self-energy might then be evaluated numerically.

III. DYNAMICAL SPIN SUSCEPTIBILITY AND SPIN-LATTICE RELAXATION

In the paramagnetic phase, the spin correlation still plays an important role in formulating the actual magnetic order in the ground states. Considering the spin fluctuations in the paramagnetic phase thus is essential. In this section, the spin fluctuations are addressed in terms of the spin-lattice relaxation time being established from the dynamical spin susceptibility function. In this manner, the spin-relaxation rate reads

$$\frac{1}{T_1} = \lim_{\omega_N \to 0} \frac{T}{N} \sum_{\mathbf{q}} |A(\mathbf{q})|^2 \frac{\text{Im}\chi(\mathbf{q},\omega_N)}{\omega_N}, \tag{11}$$

where T_1 is the spin-relaxation time, $\chi(\mathbf{q},\omega)$ is the dynamical transverse spin susceptibility function depending on momentum $\mathbf{q}$ in a system with N lattice sites, and ω_N is the Larmor frequency [38]. $A(\mathbf{q})$ in Eq. (11) is a hyperfine interaction. In the representation, $1/T_1T$ measures the slope of the imaginary part of the local spin susceptibility function $\chi_{\text{loc}} = \chi(\omega) = (1/N)\sum_{\mathbf{q}} \chi(\mathbf{q},\omega)$ in the zero-frequency limit [34]. Firstly, we would start with a calculation of the general dynamical transverse spin susceptibility that is defined as

$$\chi(\mathbf{q}, i\omega_l) = \int_0^\beta d\tau\, e^{i\omega_l\tau} \sum_j e^{i\mathbf{q}\mathbf{R}_j} \langle \mathcal{T} s^z(\mathbf{R}_j,\tau) s^z(\mathbf{0},0)\rangle, \tag{12}$$

where $\omega_l = 2\pi T l$ is a bosonic Matsubara frequency, $\mathcal{T}$ is the imaginary time order operator, and

$$s^z(\mathbf{R}_i,\tau) = \frac{1}{2}\sum_\sigma c^\dagger_{i\sigma}(\tau)\sigma c_{i\sigma}(\tau) \tag{13}$$

is the time dependence of the z component of the spin operator at lattice site i. In the infinite-dimensional limit, the general dynamical transverse spin susceptibility might be obtained

from the ladder sum in a summation over frequencies [38], such that

$$\chi(\mathbf{q}, i\omega_l) = \sum_{nn'} \tilde{\chi}_{\mathbf{q}}(i\omega_n, i\omega_{n'}; i\omega_l), \tag{14}$$

where $\tilde{\chi}_{\mathbf{q}}(i\omega_n, i\omega_{n'}; i\omega_l)$ satisfies an equation

$$\begin{aligned}\tilde{\chi}_{\mathbf{q}}(i\omega_n, i\omega_{n'} i\omega_l) &= \tilde{\chi}^0_{\mathbf{q}}(i\omega_n; i\omega_l)\delta_{nn'} \\ &+ \tilde{\chi}^0_{\mathbf{q}}(i\omega_n; i\omega_l)\frac{1}{\beta}\sum_{\sigma\sigma' n''} \Gamma^{\sigma\sigma'}(i\omega_n, i\omega_{n''}; i\omega_l) \\ &\times \tilde{\chi}_{\mathbf{q}}(i\omega_{n''}, i\omega_{n'}; i\omega_l)\sigma\sigma',\end{aligned} \tag{15}$$

in which $\tilde{\chi}^0_{\mathbf{q}}(i\omega_n; i\omega_l)$ is the bare susceptibility in the contribution of the elementary particle-hole bubble,

$$\tilde{\chi}^0_{\mathbf{q}}(i\omega_n; i\omega_l) = -\sum_{\mathbf{k}} G(\mathbf{k}, i\omega_n) G(\mathbf{k}+\mathbf{q}, i\omega_{n+l}), \tag{16}$$

and $\Gamma^{\sigma\sigma'}(i\omega_n, i\omega_{n''}; i\omega_l)$ denotes the irreducible vertex function.

In the infinite-dimensional limit ($d \to \infty$), the $\mathbf{q}$ dependence of $\tilde{\chi}^0_{\mathbf{q}}(i\omega_n; i\omega_l)$ in Eq. (16) is summarized in a single parameter $X = \sum_i \cos q_i/d$ [38,44], that reads

$$\begin{aligned}\tilde{\chi}^0_{\mathbf{q}}(i\omega_n; i\omega_l) &\equiv \tilde{\chi}^0_X(i\omega_n; i\omega_l) \\ &= \frac{-1}{\sqrt{1-X^2}} \int \frac{d\epsilon\, \rho(\epsilon)}{z_n - \epsilon} F\left(\frac{z_{n+l} - X\epsilon}{\sqrt{1-X^2}}\right),\end{aligned} \tag{17}$$

where $F(x) = \int d\epsilon\, \rho(\epsilon)/(x-\epsilon)$ is the Hilbert transform of the noninteracting density of states and $z_n = i\omega_n + \mu - \Sigma(i\omega_n)$.

The calculation of the full susceptibility requires a result of the local irreducible vertex function. In the present work, the irreducible vertex function is evaluated by using the Baym-Kadanoff approach [43,51,52]. In that scheme, in order to evaluate the spin susceptibility function, an external time-dependent magnetic field $h_\sigma(\tau)$ is added to the action. According to the presence of the external field, the Green's function and also its self-energy are not time-translation invariant in imaginary time. In other words, the self-energy and the Green's function now depend on two Matsubara frequencies [43,44]. In the Baym-Kadanoff approach, the irreducible vertex function is found as a differentiation of the self-energy with respect to the Green's function

$$\Gamma^{\sigma\sigma'}(i\omega_n, i\omega_{n'}; i\omega_l) = \frac{1}{T}\frac{\delta\Sigma_\sigma(i\omega_n, i\omega_{n+l})}{\delta G_{\sigma'}(i\omega_{n'}, i\omega_{n'+l})}. \tag{18}$$

Here, both the Green's function and the self-energy depend on two frequencies. In this sense, Eq. (12) might be rewritten to express the two-frequency Green's function $G_\sigma(i\omega_n, i\omega_m)$ as in a matrix form

$$G_\sigma(i\omega_n, i\omega_m) = \sum_{\alpha S} W_{\alpha,S}\left[Z^{\alpha S}_\sigma\right]^{-1}_{nm}, \tag{19}$$

where $[Z^{\alpha S}_\sigma]_{nm} = [\mathcal{G}_\sigma(n,m)]^{-1} - JS\sigma\alpha$. We shall restrict our discussion to the case in which only one Fourier component $l \neq 0$ of $h_\sigma(\tau)$ is nonzero. In this condition, the matrix has a nonzero diagonal $m = n$ and one nonzero off-diagonal $m + l = n$. After some tedious calculations, one finds a simple relation

$$\Sigma_\sigma(i\omega_n, i\omega_{n+l}) = \frac{\Pi^\sigma_{n,l}}{\Xi^\sigma_{n,l}} G_\sigma(i\omega_n, i\omega_{n+l}), \tag{20}$$

where

$$\begin{aligned}\Pi^\sigma_{n,l} &= \frac{\Sigma_\sigma(i\omega_n)}{2G_\sigma(i\omega_{n+l})}\left[\mathcal{G}^{-1}_\sigma(i\omega_n) + \mathcal{G}^{-1}_\sigma(i\omega_{n+l})\right] \\ &- \Sigma_\sigma(i\omega_{n+l})\left[\mathcal{G}^{-1}_\sigma(i\omega_{n+l})\right]^2 \\ &+ \frac{A_\sigma}{2G_\sigma(i\omega_n)G_\sigma(i\omega_{n+l})} + J^2\Sigma_\sigma(i\omega_{n+l})\end{aligned} \tag{21}$$

and

$$\begin{aligned}\Xi^\sigma_{n,l} &= G_\sigma(i\omega_n)\Sigma_\sigma(i\omega_n)\left[\mathcal{G}^{-1}_\sigma(i\omega_n) + \mathcal{G}^{-1}_\sigma(i\omega_{n+l})\right] \\ &+ A_\sigma + G_\sigma(i\omega_n)\left\{\left[\mathcal{G}^{-1}_\sigma(i\omega_{n+l})\right]^2 - J^2\right\},\end{aligned} \tag{22}$$

in which we have denoted

$$A_\sigma = (W_{1,-1} - W_{1,1})J\sigma. \tag{23}$$

From Eq. (20), one easily delivers a result of the irreducible vertex function by means of Eq. (18):

$$\begin{aligned}\Gamma^{\sigma\sigma'}(i\omega_n, i\omega_{n'}; i\omega_l) &= \delta_{\sigma\sigma'}\delta_{nn'}\frac{1}{T}\frac{\delta\Sigma_\sigma(i\omega_n, i\omega_{n+l})}{\delta G_\sigma(i\omega_n, i\omega_{n'+l})} \\ &= \delta_{\sigma\sigma'}\delta_{nn'}\frac{1}{T}\frac{\Pi^\sigma_{n,l}}{\Xi^\sigma_{n,l}}.\end{aligned} \tag{24}$$

The correlation function $\tilde{\chi}_{\mathbf{q}}(i\omega_n, i\omega_{n'}; i\omega_l)$ in Eq. (15) and then the dynamical transverse spin susceptibility function in Eq. (20) are simply derived. One finds

$$\chi(\mathbf{q}, i\omega_l) = T\sum_n \frac{\Xi^\sigma_{n,l}}{\Xi^\sigma_{n,l}\left[\tilde{\chi}^0_{\mathbf{q}}(i\omega_n; i\omega_l)\right]^{-1} - \Pi^\sigma_{n,l}}. \tag{25}$$

The susceptibility in Eq. (25) is expressed in the bosonic Matsubara frequency. In order to be applicable in further discussion, hereafter we would rewrite the susceptibility function in the real frequency by using the analytical continuous $i\omega_l \to \omega + i0^+$ transformation [53]. The real frequency ω-dependent susceptibility function then reads

$$\begin{aligned}\chi(\mathbf{q}, \omega) &= \int \frac{d\varepsilon}{2\pi i}[n_F(\varepsilon) - n_F(\varepsilon+\omega)]f^{AR}(\varepsilon, \varepsilon+\omega) \\ &- \int \frac{d\varepsilon}{2\pi i}[n_F(\varepsilon)f^{RR}(\varepsilon, \varepsilon+\omega) \\ &- n_F(\varepsilon+\omega)f^{AA}(\varepsilon, \varepsilon+\omega)],\end{aligned} \tag{26}$$

where $n_F(\varepsilon)$ is the Fermi-Dirac distribution function, and

$$\begin{aligned}&f^{\mu\nu}_{\mathbf{q}}(\varepsilon, \varepsilon+\omega) \\ &= \frac{\Xi^\sigma(\varepsilon, \varepsilon+\omega)}{\Xi^\sigma(\varepsilon, \varepsilon+\omega)\left[\tilde{\chi}^0_{\mathbf{q}}(\varepsilon, \varepsilon+\omega)\right]^{-1} - \Pi^\sigma(\varepsilon, \varepsilon+\omega)},\end{aligned} \tag{27}$$

with the subscripts $\mu, \nu = \{A, R\}$ (A or R refers to the advanced or retarded Green's function and self-energy) denoting for the arguments corresponding to the frequency ε being μ

and the left ones to the frequency $\varepsilon+\omega$ being ν. For instance, the $f_{\mathbf{q}}^{AR}(\varepsilon,\varepsilon+\omega)$ in Eq. (27) is established with

$$\Xi^{\sigma}(\varepsilon,\varepsilon+\omega)^{AR} = G_{\sigma}^{A}(\varepsilon)\Sigma_{\sigma}^{A}(\varepsilon)\left[\mathcal{G}_{\sigma}^{-1}(\varepsilon)^{A}+\mathcal{G}_{\sigma}^{-1}(\varepsilon+\omega)^{R}\right] + A_{\sigma}+G_{\sigma}^{A}(\varepsilon)\left\{\left[\mathcal{G}_{\sigma}^{-1}(\varepsilon+\omega)^{R}\right]^{2}-J^{2}\right\}, \tag{28}$$

$$\Pi^{\sigma}(\varepsilon,\varepsilon+\omega)^{AR} = \frac{\Sigma_{\sigma}^{A}(\varepsilon)}{2G_{\sigma}^{R}(\varepsilon+\omega)}\left[\mathcal{G}_{\sigma}^{-1}(\varepsilon)^{A}+\mathcal{G}_{\sigma}^{-1}(\varepsilon+\omega)^{R}\right] - \Sigma_{\sigma}^{R}(\varepsilon+\omega)\left[\mathcal{G}_{\sigma}^{-1}(\varepsilon+\omega)^{R}\right]^{2} + \frac{A_{\sigma}}{2G_{\sigma}^{A}(\varepsilon)G_{\sigma}^{R}(\varepsilon+\omega)}+J^{2}\Sigma_{\sigma}^{R}(\varepsilon+\omega), \tag{29}$$

and

$$\tilde{\chi}_{\mathbf{q}}^{0}(\varepsilon,\varepsilon+\omega)^{AR} = \frac{-1}{\sqrt{1-X^{2}}}\int\frac{d\epsilon\,\rho(\epsilon)}{\varepsilon-i0^{+}+\mu-\Sigma^{A}(\varepsilon)-\epsilon} \times F\left(\frac{\varepsilon+\omega+i0^{+}+\mu-\Sigma^{R}(\varepsilon+\omega)-X\epsilon}{\sqrt{1-X^{2}}}\right). \tag{30}$$

For the low-frequency limit, the spin susceptibility function might be expanded to the first order of ω and by noting that $(f_{\mathbf{q}}^{AA})^{*}=f_{\mathbf{q}}^{RR}$, one would deliver a simple expression of the susceptibility function

$$\chi(\mathbf{q},\omega)=\omega\int\frac{d\varepsilon}{2\pi i}\frac{\partial n_{F}(\varepsilon)}{\partial\varepsilon}\left[f_{\mathbf{q}}^{AR}(\varepsilon,\varepsilon)-f_{\mathbf{q}}^{RR}(\varepsilon,\varepsilon)\right]. \tag{31}$$

In the infinite-dimensional limit $d\to\infty$, the local dynamical spin susceptibility $\chi(\omega)=\sum_{\mathbf{q}}\chi(\mathbf{q},\omega)/N$ can be evaluated as for the "generic" case, i.e., we have an identity $\chi(\omega)=\chi(X=0,\omega)$ [38]. That leads us to a more simple expression to evaluate the spin-relaxation time. Indeed, Eq. (11) can be rewritten in the following way:

$$\frac{1}{T_{1}T}=A^{2}\mathrm{Im}\int\frac{d\varepsilon}{2\pi i}\frac{\partial n_{F}(\varepsilon)}{\partial\varepsilon}\left[f_{\mathrm{loc}}^{AR}(\varepsilon,\varepsilon)-f_{\mathrm{loc}}^{RR}(\varepsilon,\varepsilon)\right], \tag{32}$$

where $f_{\mathrm{loc}}^{\mu\nu}(\varepsilon,\varepsilon)$ has been replaced for $f_{\mathbf{q}}^{\mu\nu}(\varepsilon,\varepsilon)$ in Eq. (27) in the case of the generic situation. In this case, the bare susceptibility function simply reads $\tilde{\chi}_{X=0}^{0}(\varepsilon,\varepsilon)=-G_{\sigma}(\varepsilon)G_{\sigma}(\varepsilon)$ [38]. The hyperfine interaction here has been considered as locally $A(\mathbf{q})\equiv A$.

IV. NUMERICAL RESULTS

In order to analyze the spin-relaxation process in DMSs, firstly we discuss the signatures of the dynamical spin susceptibility. By solving self-consistently the set of equations in Eqs. (2), (4), and (10), one finds solutions to the local Green's function and its respective self-energy as functions of frequency. The dynamical spin susceptibility is then easily evaluated following Eq. (31).

In Fig. 1, we show the signatures of the imaginary part of the local dynamical spin susceptibility function for different carrier densities n at a given set of parameters with $J=4$, $x=0.1$, and $T=0.1$. In the set of parameters, the system settles in the PM state. For a fixed value of the carrier density n, the susceptibility always shows a single peak at low frequency. The peak indicates the fluctuations of the local moments in the PM state. As increasing the carrier density, the peak shifts to a higher frequency; however, the height of the peak becomes maximum at $n=x/2$ corresponding to the half-filled impurity band situation. Indeed, in this case with the large magnetic coupling, a critical temperature for the PM-FM transition in the system becomes maximum [8,21]. That means, by lowering the temperature from the PM state, the magnetic fluctuations in the case of the half-filled impurity band become enlarged in comparison with others. Note here that the resonance peak in the local dynamical spin susceptibility also analyzes the magnetic coherence occurring in the diluted systems and the quasiparticle lifetime is in the order of the height of the peak. The magnetic coherence thus is the most favored in this half-filled impurity band case. At low carrier density, the magnetic coupling plays an important role to all of the carriers that establish energetically the magnetic bound state. Increasing the carrier density, on average, the carriers lose their magnetic correlations with the local moments. The bound coherence energy thus is suppressed and the total magnetic fluctuations in the systems are restrained. The peak in the local dynamical spin susceptibility thus shifts to the right with higher frequency as shown in Fig. 1.

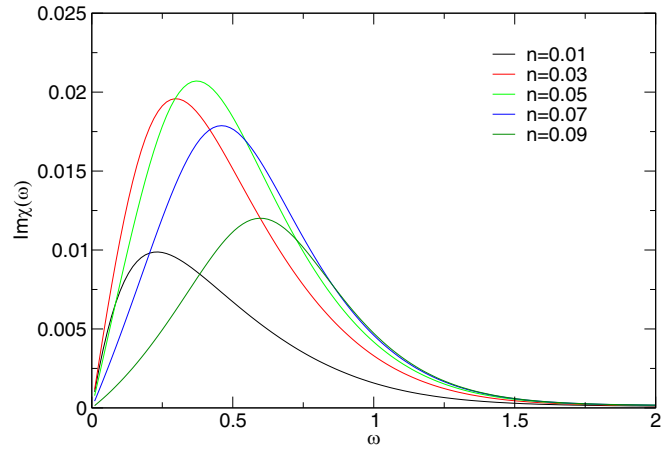

FIG. 1. Imaginary part of the local dynamical spin susceptibility for different carrier densities with $J=4$ and $x=0.1$ at $T=0.1$.

To discuss in more detail the magnetic resonance in the case of the half-filled impurity band, we show in Fig. 2 the imaginary part of the local dynamical spin susceptibility function at $J=4$, $x=0.1$, and $n=0.05$ for several temperatures. Note here that, in the range of temperature, the system settles in the PM state and the analytical calculation for the local dynamical spin susceptibility function in Eq. (31) is still applicable. At a given temperature, one always finds a single low-frequency peak structure in the local dynamical spin susceptibility function indicating the magnetic coherence effect in the system. At a low temperature very close to the PM-FM transition point, the local dynamical spin susceptibility gets a sharp peak at low frequency. In this case, as increasing the temperature, the thermal fluctuations destroy the coherence effect resulting in height depression of the peak. The thermal fluctuations, in addition, lose the magnetic bound state between the carrier and the local moments. The peak

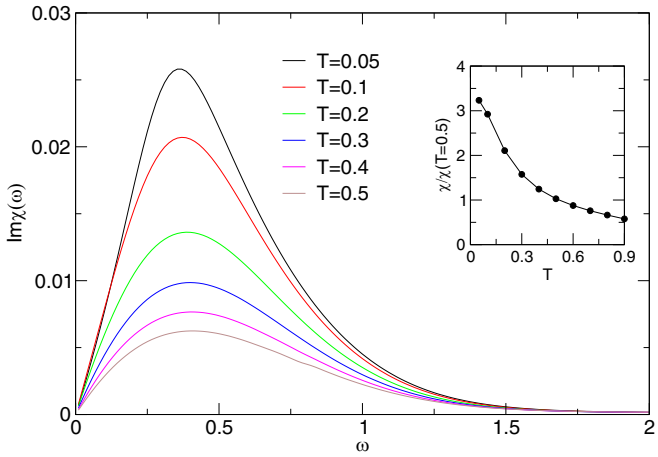

FIG. 2. Imaginary part of the local dynamical spin susceptibility at different temperatures with $n = 0.05$ and $x = 0.1$ at $J = 4$. The inset shows the static spin susceptibility function versus temperature for the same set of parameters in the main figure.

thus shifts to the right with higher frequency once increasing the temperature. The behaviors of the local dynamical spin susceptibility also address the possibility of the spin clusters at low temperature with the characteristic size approximating to the static spin susceptibility. That is indicated by the dramatic increase of the dynamical spin susceptibility at low frequency once the temperature reaches the critical temperature of the PM-FM transition. In the inset of Fig. 2 we show the behavior of the static susceptibility function χ established by the sum rule for the imaginary part of the dynamical spin susceptibility function: $\int d\omega \, \mathrm{Im}\chi(\omega)/(2\pi\omega) = \chi$ [54,55]. Apparently, the static susceptibility obeys the Curie law $\chi \sim 1/T$ for large temperature T [56].

To inspect in more detail the spin fluctuations, and especially, the spin-relaxation process, we address in Fig. 3 the spin-relaxation rate $1/T_1$ depending on the temperature at $J = 4$ for some values of n at $x = 0.1$. At a given carrier

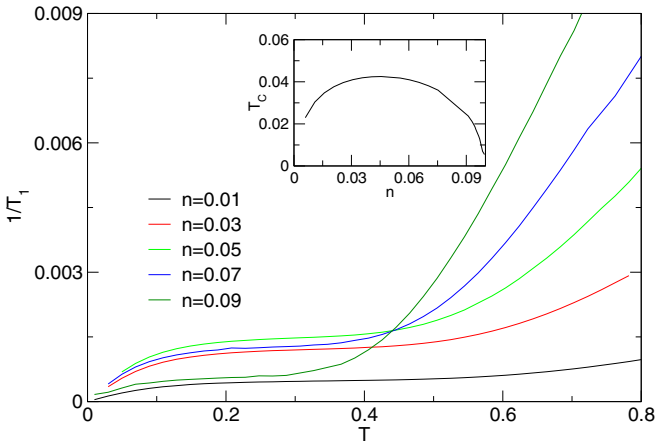

FIG. 3. Spin-lattice relaxation rate as a function of temperature at $J = 4$ for some values of n at $x = 0.1$ in the unit of A^2. The inset shows the PM-FM transition temperature T_C versus carrier density n at $J = 4$ and $x = 0.1$ [21,22].

density n, one always finds a monotonous increase of the spin-relaxation rate as increasing temperature. The increase in the temperature is commonly associated with the thermally activated acceleration of internal motion, decreasing the correlation time under the fast motion due to the thermal fluctuations. In a large temperature range, the spin-relaxation rate is linearly proportional to the temperature indicating that the strong thermal fluctuations have depressed the magnetic correlations and the system behaviors as for the conventional paramagnetic metals. In that condition, the spin-lattice relaxation is dominated by a Korringa process in which the relaxing nuclear spin flips an electronic spin down. By lowering the temperature the spin-relaxation rate slows down and the linear dependence of the spin-relaxation rate versus temperature is replaced by the exponential dependence. In this temperature range, despite the likely metallic state, the system probably returns to the unconventional metal due to reinforcing the spin fluctuations. In such a region, with the development of FM correlations upon cooling, the system generally generates nonuniform magnetization, which causes a formation of the spin clusters close to the PM-FM transition point. Approaching the critical temperature from higher temperatures, the FM coupling progressively develops and the FM ordering strengthens, which facilitates the enhancement of the spin-relaxation time or sharply suppresses the spin-relaxation rate as shown in Fig. 3.

In DMSs, the conductance is achieved by the hole hopping via the exchange-coupled localized spins, that carriers make mediate the relaxation of the exchange-coupled localized moments to the lattice. By depressing the thermal fluctuations, the mobility of the carriers is reduced resulting in the localization of carriers. The formation of polarons with the spin clusters in DMSs thus can be released in the signatures of the spin-relaxation rates in our study. Increasing the carrier density as discussed above, the carriers feel they are losing magnetic correlations with the localized moments, consequently reinforcing the mobility of the hole carriers. The spin-relaxation rate thus rapidly increases as increasing the carrier density in the large temperature regime, as expected in Korringa scaling [24,57]. The scenario completely differs in the lower temperatures, e.g., $T < 0.4$, in which the spin-relaxation rate is not in the order of T due to the strongly magnetic correlations. Indeed, the spin-relaxation rate in the regime increases as increasing carrier density and then decreases if the impurity band deviates from the half-filling case. By lowering the temperature, the thermal fluctuations more and more play a less important role and the magnetic correlations become dominated. The mobility of the hole carriers is now primarily mediated by the magnetic coupling between the carriers and the localized moments. With large magnetic coupling, the mobility is largest at the half-filling impurity band that dominates the spin-relaxation rate. The spin-relaxation rate then diminishes once the filling of the impurity band deviates from the half-filling case.

To discuss the magnetic coupling influence in the spin-relaxation process in the case of the half-filling impurity band, we present in Fig. 4 the spin-relaxation rate versus temperature for different values of J at $x = 0.1$ and $n = 0.05$. For a fixed value of the magnetic coupling, one always finds the linear dependence of the spin-relaxation rate if the tempera-

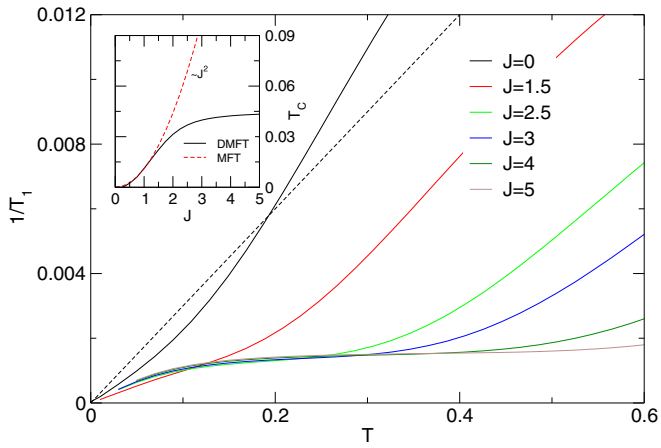

FIG. 4. Spin-lattice relaxation rate $1/T_1$ as a function of temperature for some values of J at $x = 0.1$ and $n = 0.05$ in the unit of A^2. The black dashed line addresses $1/T_1$ versus T for a three-dimensional free electron gas with hyperfine coupling. The inset shows the PM-FM transition temperature T_C versus magnetic coupling J at $x = 0.1$ and $n = 0.05$. The red dashed line in the inset is T_C as a function of J found in the standard MFT. It expresses the J^2 rule.

ture is sufficiently large. Once the magnetic coupling is small, the linear behavior indicating the metallic-like state emerges even at low temperatures. Specifically, for $J = 0$, i.e., a noninteracting fermion system, the spin-relaxation rate versus temperature shows approximately the linear behavior in the whole temperature range. That evidence typifies the Korringa process in normal metals driven only by hyperfine interaction [24,25]. The exponential dependence of the spin-relaxation rate on low temperature appears only if the magnetic coupling is strong enough, e.g., $J > 2$. In this case, the impurity band due to the magnetic doping starts separating to the main band of the semiconductor. The separation becomes stabilized once $J \geqslant 3$ [8,21,41]. In the case of the half-filling impurity band, the mobility of the carriers is mediated by the magnetic correlation that favors the magnetic coherence bound state or the spin cluster formation for temperature approaching the FM critical transition point with respect to the sharp suppression of the spin-relaxation rate at low temperature in the large magnetic coupling cases. The sharp suppression of the spin-relaxation rate or the speeding up of the spin-relaxation time can be attributed to the appearance of the magnetic coherence bound state or the spin clusters while approaching the FM order. The FM correlation length in the PM phase is enlarged as increasing the magnetic coupling as observed in similar materials of doped manganites even well above the PM-FM transition temperature [58,59]. To verify our theoretical study in describing the DMS magnetic properties, we show in the inset of Fig. 4 the critical temperature T_C versus magnetic coupling J. The critical PM-FM transition temperature is addressed both in the standard mean-field approximation (MFA) applied for the general Zener model (red dashed line) [2,6,60] and the DMFT applied for the simplified Hamiltonian in Eq. (1) (black solid line) for the same set of parameters. Apparently, at low temperatures and small magnetic coupling, the correlations become less important and the result of MFA converges to that evaluated by DMFT. In the case of large magnetic coupling, the critical temperature evaluated by MFA becomes overestimated. The spin-relaxation rate evaluated in a three-dimensional noninteracting electron gas also well agrees with our result for $J = 0$ at least in the very low temperature range (see black dashed line in the main panel). For larger temperatures, the two results do not fit each other. The discrepancy comes from the rough assumption, as in the literature, that the Korringa relation $1/T_1 \sim |A\chi|^2 T$ is specified with the uniform susceptibility $\chi \sim \rho(E_F)$, where $\rho(E_F)$ is the density of states at the Fermi level estimated at zero temperature [24,25,61]. However, in general, χ or the density of states is temperature dependent. In our DMFT calculation, the nuclear spin-lattice relaxation rate $1/T_1$ is evaluated originally from Eq. (11) even for $J = 0$, so all temperature dependence is taken into account resulting in the deviation of the spin-relaxation rate from its Korringa law.

V. CONCLUSION

To conclude, we have discussed the low-frequency spin dynamic scenario in paramagnetic diluted magnetic semiconductors within the dynamical mean field theory. In the infinite-dimensional limit, we derive a set of self-consistent equations so the single-particle Green's function and its self-energy of the Kondo lattice model can be evaluated numerically. These results permit us to inspect the spin dynamic properties in the system by analyzing the local dynamical spin susceptibility function and the spin-relaxation rate. It is found that the spin fluctuations become dominated, indicated by the sharp peak appearing at a low frequency of the spin dynamical susceptibility function in the case of large magnetic coupling and temperature close to the paramagnetic-ferromagnetic transition point. The low-frequency spin dynamics in the systems is also addressed in the signatures of the spin-relaxation process. In the case of large temperature and small magnetic coupling, the spin-relaxation rate releases the scenario of the Korringa process specifying the weak correlation systems likely normal metals. Otherwise, i.e., at small temperature and large magnetic coupling, we find exponential behavior of the spin-relaxation rate versus temperature. Moreover, at a temperature approaching the paramagnetic-ferromagnetic transition point, one finds the sharp suppression of the spin-relaxation rate or the speeding up of the spin-relaxation time. These scenarios are attributed to the appearance of the magnetic coherence bound state or the spin clusters in DMSs due to the strongly magnetic correlations. The random distribution of magnetic ions actually reduces the ferromagnetic-paramagnetic transition temperature in a doped magnetic system. Studying the influence of the magnetic random distribution to the spin-relaxation signatures in DMSs thus is essential and will be left for near future studies.

ACKNOWLEDGMENT

This research is funded by the Vietnam National Foundation for Science and Technology Development (NAFOSTED) under Grant No. 103.01-2019.306.

[1] T. Jungwirth, J. Wunderlich, V. Novák, K. Olejník, B. L. Gallagher, R. P. Campion, K. W. Edmonds, A. W. Rushforth, A. J. Ferguson, and P. Němec, Rev. Mod. Phys. **86**, 855 (2014).
[2] T. Dietl and H. Ohno, Rev. Mod. Phys. **86**, 187 (2014).
[3] T. Dietl, Semicond. Sci. Technol. **17**, 377 (2002).
[4] T. Dietl, A. Haury, and Y. Merle d'Aubigné, Phys. Rev. B **55**, R3347 (1997).
[5] P. J. T. Eggenkamp, H. J. M. Swagten, T. Story, V. I. Litvinov, C. H. W. Swüste, and W. J. M. de Jonge, Phys. Rev. B **51**, 15250 (1995).
[6] T. Jungwirth, J. Sinova, J. Mašek, J. Kučera, and A. H. MacDonald, Rev. Mod. Phys. **78**, 809 (2006).
[7] T. Dietl, H. Ohno, F. Matsukura, J. Cibert, and D. Ferrand, Science **287**, 1019 (2000).
[8] A. Chattopadhyay, S. Das Sarma, and A. J. Millis, Phys. Rev. Lett. **87**, 227202 (2001).
[9] A. Kaminski and S. Das Sarma, Phys. Rev. B **68**, 235210 (2003).
[10] S. Das Sarma, E. H. Hwang, and A. Kaminski, Phys. Rev. B **67**, 155201 (2003).
[11] V. M. Galitski, A. Kaminski, and S. Das Sarma, Phys. Rev. Lett. **92**, 177203 (2004).
[12] A. Kaminski, V. M. Galitski, and S. Das Sarma, Phys. Rev. B **70**, 115216 (2004).
[13] T. Dietl, Nat. Mater. **9**, 965 (2010).
[14] W. Nolting, Phys. Status Solidi B **96**, 11 (1979).
[15] G. Tang and W. Nolting, Phys. Rev. B **75**, 024426 (2007).
[16] G. R. Stewart, Rev. Mod. Phys. **56**, 755 (1984).
[17] W. Nolting, T. Hickel, A. Ramakanth, G. G. Reddy, and M. Lipowczan, Phys. Rev. B **70**, 075207 (2004).
[18] V. Bryksa and W. Nolting, Phys. Rev. B **78**, 064417 (2008).
[19] A. Schwabe and W. Nolting, Phys. Rev. B **80**, 214408 (2009).
[20] V.-N. Phan and M.-T. Tran, Phys. Rev. B **92**, 155201 (2015).
[21] D.-H. Bui, Q.-H. Ninh, H.-N. Nguyen, and V.-N. Phan, Phys. Rev. B **99**, 045123 (2019).
[22] V.-N. Phan and H.-N. Nguyen, Phys. Rev. B **102**, 125202 (2020).
[23] P. Nyhus, S. Yoon, M. Kauffman, S. L. Cooper, Z. Fisk, and J. Sarrao, Phys. Rev. B **56**, 2717 (1997).
[24] J. Korringa, Physica **16**, 601 (1950).
[25] C. P. Slichter, *Principles of Magnetic Resonance* (Springer, Berlin, 1990).
[26] E. Souto, O. Nunes, and A. Fonseca, Solid State Commun. **129**, 605 (2004).
[27] D. Scalbert, Phys. Status Solidi B **193**, 189 (1996).
[28] D. Scalbert, J. Cernogora, and C. A La Guillaume, Solid State Commun. **66**, 571 (1988).
[29] I. V. Krainov, V. F. Sapega, N. S. Averkiev, G. S. Dimitriev, K. H. Ploog, and E. Lähderanta, Phys. Rev. B **92**, 245201 (2015).
[30] I. V. Krainov, V. F. Sapega, G. S. Dimitriev, and N. S. Averkiev, J. Phys.: Condens. Matter **33**, 445802 (2021).
[31] T. Pruschke, M. Jarrell, and J. Freericks, Adv. Phys. **44**, 187 (1995).
[32] T. Story, C. H. W. Swüste, P. J. T. Eggenkamp, H. J. M. Swagten, and W. J. M. de Jonge, Phys. Rev. Lett. **77**, 2802 (1996).
[33] M. Jarrell and T. Pruschke, Phys. Rev. B **49**, 1458 (1994).
[34] R. Žitko, Ž. Osolin, and P. Jeglič, Phys. Rev. B **91**, 155111 (2015).
[35] X. Chen, J. P. F. LeBlanc, and E. Gull, Nat. Commun. **8**, 14986 (2017).
[36] J. Mußhoff, A. Kiani, and E. Pavarini, Phys. Rev. B **103**, 075136 (2021).
[37] N. Bulut, D. W. Hone, D. J. Scalapino, and N. E. Bickers, Phys. Rev. B **41**, 1797 (1990).
[38] A. Georges, G. Kotliar, W. Krauth, and M. J. Rozenberg, Rev. Mod. Phys. **68**, 13 (1996).
[39] O. Akerlund, P. de Forcrand, A. Georges, and P. Werner, Phys. Rev. D **88**, 125006 (2013).
[40] U. Schneider, L. Hackermueller, S. Will, T. Best, I. Bloch, T. A. Costi, R. W. Helmes, D. Rasch, and A. Rosch, Science **322**, 1520 (2008).
[41] E. H. Hwang and S. DasSarma, Phys. Rev. B **72**, 035210 (2005).
[42] I. D. Marco, P. Thunström, M. I. Katsnelson, J. Sadowski, K. Karlsson, S. Lebègue, J. Kanski, and O. Eriksson, Nat. Commun. **4**, 2645 (2013).
[43] J. K. Freericks and P. Miller, Phys. Rev. B **62**, 10022 (2000).
[44] J. K. Freericks and V. Zlatić, Rev. Mod. Phys. **75**, 1333 (2003).
[45] O. M. Fedorych, E. M. Hankiewicz, Z. Wilamowski, and J. Sadowski, Phys. Rev. B **66**, 045201 (2002).
[46] M. Takahashi, Materials **3**, 3740 (2010).
[47] N. Furukawa, J. Phys. Soc. Jpn. **63**, 3214 (1994).
[48] N. Furukawa, J. Phys. Soc. Jpn. **64**, 2754 (1995).
[49] N. Furukawa, J. Phys. Soc. Jpn. **65**, 1174 (1996).
[50] N. Furukawa, in *Physics of Manganites*, edited by T. A. Kaplan and S. D. Mahanti, Fundamental Materials Research (Kluwer, New York, 1999), p. 1.
[51] G. Baym and L. P. Kadanoff, Phys. Rev. **124**, 287 (1961).
[52] G. Baym, Phys. Rev. **127**, 1391 (1962).
[53] H. Bruus and K. Flensberg, *Many-Body Quantum Theory in Condensed Matter Physics* (Oxford University Press, New York, 2004).
[54] P. C. Hohenberg and W. F. Brinkman, Phys. Rev. B **10**, 128 (1974).
[55] J. Yoshitake, J. Nasu, and Y. Motome, Phys. Rev. Lett. **117**, 157203 (2016).
[56] A. Shengelaya, G.-m. Zhao, H. Keller, and K. A. Müller, Phys. Rev. Lett. **77**, 5296 (1996).
[57] D. Kölbl, D. M. Zumbühl, A. Fuhrer, G. Salis, and S. F. Alvarado, Phys. Rev. Lett. **109**, 086601 (2012).
[58] V. A. Atsarkin, V. V. Demidov, F. Simon, R. Gaal, Y. Moritomo, K. Conder, A. Jánossy, and L. Forró, J. Magn. Magn. Mater. **258-259**, 256 (2003).
[59] M. S. Seehra and R. P. Gupta, Phys. Rev. B **9**, 197 (1974).
[60] A. Kassaian and M. Berciu, Phys. Rev. B **71**, 125203 (2005).
[61] B. S. Shastry and E. Abrahams, Phys. Rev. Lett. **72**, 1933 (1994).